NASA TECHNICAL NOTE

NASA TN D-8077

NASA TN D-8077

COMPUTER SIMULATION OF AN AIRCRAFT-BASED DIFFERENTIAL ABSORPTION AND SCATTERING SYSTEM FOR RETRIEVAL OF SO_2 VERTICAL PROFILES

James M. Hoell, Jr.

Langley Research Center
Hampton, Va. 23665

NATIONAL AERONAUTICS AND SPACE ADMINISTRATION • WASHINGTON, D. C. • DECEMBER 1975

1 Report No	2 Government Accession No	3 Recipient's Catalog No
NASA TN D-8077		

4 Title and Subtitle	5 Report Date
COMPUTER SIMULATION OF AN AIRCRAFT-BASED DIFFERENTIAL ABSORPTION AND SCATTERING SYSTEM FOR RETRIEVAL OF SO_2 VERTICAL PROFILES	December 1975
	6 Performing Organization Code

7 Author(s)	8 Performing Organization Report No
James M. Hoell, Jr.	L-10398
	10 Work Unit No
9 Performing Organization Name and Address	176-21-31-09
NASA Langley Research Center Hampton, Va. 23665	11 Contract or Grant No
	13 Type of Report and Period Covered
12 Sponsoring Agency Name and Address	Technical Note
National Aeronautics and Space Administration Washington, D.C. 20546	14 Sponsoring Agency Code

15 Supplementary Notes

16 Abstract

The feasibility of using the differential absorption and scattering technique from aircraft altitudes for remotely measuring the vertical distribution of SO_2 is studied via a computer simulation. Particular care is taken in this simulation to use system parameters (i.e., laser energy, telescope size, etc.) which can be accommodated on an aircraft and can be realized with commercially available technology. The vertical molecular and aerosol profiles are chosen to simulate the types of profiles which might be experienced over a large city. Results are presented on the retrieval of the assumed SO_2 profile which show the effects of systematic errors due to interfering gases and aerosols, as well as random errors due to shot noise in the return signal, detector and background noise, and instrument-generated noise.

17 Key Words (Suggested by Author(s))	18 Distribution Statement
Ultraviolet differential absorption Remote measurement of SO_2	Unclassified – Unlimited Subject Category 45

19 Security Classif (of this report)	20 Security Classif (of this page)	21 No of Pages	22 Price*
Unclassified	Unclassified	33	$3.75

*For sale by the National Technical Information Service, Springfield, Virginia 22161

COMPUTER SIMULATION OF AN AIRCRAFT-BASED DIFFERENTIAL ABSORPTION AND SCATTERING SYSTEM FOR RETRIEVAL OF SO_2 VERTICAL PROFILES

James M. Hoell, Jr.
Langley Research Center

SUMMARY

An analysis of the feasibility of using a differential absorption and scattering (DAS) system to retrieve vertical SO_2 profiles from various aircraft altitudes is presented The analysis utilizes a computer model which simulates measured return signals for several different atmospheric conditions. From these measured signals the SO_2 column content from the platform down to various altitude levels and the SO_2 concentration averaged over the vertical resolution of the system are determined and compared with the respective true values as determined from the input profile. Particular care is taken to characterize the DAS system with parameters that can be realized by using commercially available components. The vertical molecular and aerosol profiles are chosen to simulate types of profiles which might be experienced over a large city.

Results of the simulated retrieval are presented for five different line pairs, a platform altitude of 2625 meters, and a resolution length of 500 meters. For each case considered, a systematic error and a random error are determined. The systematic error is due to an inherent difference in the return signals for the two transmitted wavelengths. The random error includes effects due to shot noise in the return signal, background noise, detector noise, and instrument noise. Effects due to scintillation and spatial averaging of the various molecule and aerosol profiles are avoided by considering only "single-shot" retrievals.

Results from this analysis indicate that the measurement of the vertical distribution of SO_2, as well as the column content from an aircraft platform, is well within the capability of the DAS techniques. Moreover, construction of a system capable of such measurement is well within present day technology.

INTRODUCTION

Differential absorption and scattering (DAS) is an active laser technique for remotely measuring atmospheric pollution which attempts to combine the high sensitivity of resonance absorption and the range-resolved capability of lidar systems. The application of the absorption technique is implemented in a DAS system through use of a pulsed laser operating on and

off of a characteristic molecular absoprtion peak. The use of standard lidar techniques permits the measurement of the backscattered energy from each transmitted wavelength as a function of range. The gas concentration is then related to the difference in the backscattered energy for each wavelength.

The first demonstration of the DAS technique (ref. 1) utilized a temperature-tuned ruby laser to measure tropospheric water vapor. (Note that an earlier application of the DAS technique to measure water vapor was reported in ref. 2; however, the light source was a xenon searchlight rather than a laser.) Results from other ground-based DAS systems have been reported in reference 3 for the measurement of atmospheric NO_2 and in references 4 and 5 for the measurement of NO_2, O_3, and SO_2 contained in a large calibration chamber. In addition to these experimental results, a number of analytical studies covering various aspects of the DAS technique have appeared in the literature. For example, a study comparing the DAS, Raman, and fluorescence techniques was reported in reference 6. The problem of uncertainty prediction for DAS has been investigated with varying degrees of sophistication in references 7, 8, 9, 10, and 11. In general, both the experimental and analytical studies have indicated that the DAS technique is capable of yielding high sensitivity for concentration and ranges useful for remote pollution monitoring with measurement errors compatible with concentration measurement needs. An important mode of operation for a DAS system, particularly for regional monitoring, is from an aircraft platform. The work reported in references 7, 8, and 9 has been oriented toward analysis of ground-based systems; of these references, measurement of SO_2 is considered only in reference 8. Measurement of SO_2 is not considered in reference 10. The present study represents the first detailed evaluation of the DAS scheme for regional monitoring of SO_2 from an aircraft-based system.

In particular, the purpose of this study is to evaluate the ability of a given aircraft-based system to "measure" various SO_2 vertical profiles. The measured profiles are constructed from a set of simulated return signals calculated by a computer model which is designed to reproduce effects of ozone and various aerosol distributions as well as background and system-generated noise. The effects of systematic errors due to interfering gases and aerosols, as well as of random errors, on the retrieval of the pollutant profile are considered. In addition, particular care has been taken in this simulation to use parameters (i.e., laser energy, filter bandwidth, telescope size, etc.) which can be accommodated on an aircraft platform and, more importantly, which can be realized with commercially available technology. Furthermore, the vertical molecular and aerosol profiles which have been used in this study were chosen to simulate the types of profiles which might be experienced over a large city.

SYMBOLS

A area of receiver, m^2

c speed of light

h	Planck's constant
$M_{k,j}$	column content of gas k from R_P down to R_j, atm-cm
$M'_{k,J}$	estimate of $M_{k,j}$, atm-cm
N_i	$= N_{1,b} + N_{1,d}$, photons/pulse
$N_{1,b}$	background noise at wavelength λ_i, photons/pulse
$N_{1,d}$	photomultiplier dark noise at wavelength λ_i, photons/pulse
n_k	molecular concentration of gas k, atm-cm-m^{-1}
n_m	atmospheric molecular density, m^{-3}
$\bar{n}_k$	spatial average of n_k, atm-cm-m^{-1}
$\bar{n}'_k$	estimate of $\bar{n}_k$, atm-cm-m^{-1}
$P_{1,J}$	return signal for λ_1 from altitude R_j, photons/pulse
Q	electronic amplification
R_J	altitude of atmospheric cell J, m
ΔR	$= R_{J+1} - R_j$, m
R_P	platform altitude, m
$S_{1,j}$	$= P_{i,J} + N_1$, photons/pulse
U_1	transmitted energy at wavelength λ_1, J
$\beta_{1,J}$	total volume backscattering coefficient for Rayleigh and Mie scattering for wavelength λ_1 and atmospheric cell J, $(m\text{-}sr)^{-1}$
β_r	volume backscattering coefficient for Rayleigh scattering, $(m\text{-}sr)^{-1}$

δ uncertainty in the parameter it precedes

η optical transmission

λ_1 wavelength, nm

ξ_i total extinction coefficient for Rayleigh and Mie scattering for wavelength λ_i, m^{-1}

ξ_r extinction coefficient for Rayleigh scattering, m^{-1}

$\sigma_{k,1}$ molecular absorption coefficient at λ_1 for gas k, $(atm\text{-}cm)^{-1}$

τ gate interval, sec

DISCUSSION OF MODEL AND SIMULATION

Figure 1 indicates the major features of a DAS system. The laser transmitter is operated at two wavelengths, λ_1 and λ_2, which are chosen to coincide with a maximum and minimum, respectively, in the absorption spectrum of the particular atmospheric constituent. Using the range gating techniques that are associated with single-ended lidar systems, the backscattered energy from a given atmospheric volume at range $R_P - R_j$ is measured for each transmitted wavelength. The backscattered energy measured at the receiver is given by the following equation.

$$P_{i,j} = \eta\left(\frac{c\tau}{2}\right)\beta_{1,j}\frac{\lambda_1}{hc}\frac{AU_1}{(R_P - R_j)^2}\exp\left(-2\int_{R_P}^{R_j}\xi_1 dr - 2\sum_k\int_{R_P}^{R_j}\sigma_{k,i}n_k dr\right) \quad (1)$$

The summation in the exponential function is over all constituents which absorb at the transmitted wavelength.

The backscattered energy is due to Rayleigh and Mie scattering of the transmitted laser energy within the atmospheric volume under observation. Because of the choice of transmitted wavelengths, the major contribution to the difference in the backscattered energies at λ_1 and λ_2 is due to the amount of absorbing gas between the transmitter and scattering volume. Consequently, a comparison of the return signals $P_{1,j}$ and $P_{2,j}$ provides a measure of the average pollutant concentration (i.e., column content) between the transmitter and the scattering volume, that is,

$$M_{1,j} = \frac{1}{2(\sigma_{1,1} - \sigma_{1,2})} \left\{ \ln\left(\frac{P_{1,j}/U_1\lambda_1}{P_{2,j}/U_2\lambda_2}\right) + \ln\left(\frac{\beta_{2,j}}{\beta_{1,j}}\right) + 2 \int_{R_P}^{R_j} \left[(\xi_1 - \xi_2) + (\sigma_{2,1} - \sigma_{2,2}) n_2 \right] dr \right\} \quad (2)$$

where

$$M_{1,j} = \int_{R_P}^{R_j} n_1 dr$$

In equation (2), the analysis has been explicitly restricted to two absorbing gases with n_1 being SO_2 and n_2 being O_3. By obtaining the column content for successive ranges, the average pollutant concentration between scattering cells can be determined from equation (3a) or (3b), which are

$$\bar{n}_1 = \frac{M_{1,j} - M_{1,j+1}}{\Delta R} \quad (3a)$$

$$\bar{n}_1 = \frac{1}{2\Delta R(\sigma_{1,1} - \sigma_{1,2})} \left\{ \ln\left(\frac{P_{1,j}P_{2,j+1}}{P_{2,j}P_{1,j+1}}\right) + \ln\left(\frac{\beta_{2,j}\beta_{1,j+1}}{\beta_{1,j}\beta_{2,j+1}}\right) + 2 \int_{R_{j+1}}^{R_j} \left[(\xi_1 - \xi_2) - (\sigma_{2,1} - \sigma_{2,2}) n_2 \right] dr \right\} \quad (3b)$$

The expressions given for the column content (eq. (2)) and average concentrations (eq. (3a) or (3b)) are exact and are based on the assumption that all parameters are either known or can be determined during a given measurement. In practice, this is generally not the case, since equations (2) and (3b) contain variables associated with the atmosphere (i.e., $\beta_{i,j}$, ξ_1, and n_k) which are not adequately known. Further complicating the use of these expressions is the fact that the signal measured at the receiver $S_{1,j}$ is the sum of the laser backscattered energy $P_{i,j}$ and noise energy N_1 due to solar background and system noise. Consequently, in an operational system, the exact equations for column content and average concentrations are replaced by the following equations:

$$M'_{1,j} = \frac{1}{2(\sigma_{1,1} - \sigma_{1,2})} \ln\left[\frac{(S_{1,j} - N_1)(U_2\lambda_2)}{(S_{2,j} - N_2)(U_1\lambda_1)}\right] \quad (4)$$

$$\bar{n}'_1 = \frac{M'_{1,j} - M'_{1,j+1}}{\Delta R} \quad (5)$$

Note that equations (4) and (5) contain only parameters which can be measured. Moreover, it should be emphasized that $M'_{1,J}$ and $\bar{n}'_1$ represent an estimate of $M_{1,J}$ and $\bar{n}_1$, and the accuracy of this estimate depends upon the choice of wavelengths as well as the atmospheric conditions during a measurement.

The basic methodology used to evaluate the performance of a given DAS system consists of comparing a retrieval or measured SO_2 profile, containing calculated measurement errors, and the "true" SO_2 profile. The true SO_2 profile can be determined from equations (2) and (3) or, directly, by averaging the assumed vertical SO_2 profile over the vertical resolution of the DAS system. The measured profiles were calculated from equations (4) and (5). One type of error considered, the systematic error, is the difference between $M_{k,J}$ and $M'_{k,j}$ and between $\bar{n}_k$ and $\bar{n}'_k$ for the column content and range-resolved concentration measurements, respectively. The systematic error is equivalent to the SO_2 column content or concentration that would be inferred from a given DAS measurement even if no SO_2 were in the measurement path. The other type of error considered is due to the random uncertainties in the measured signal. The random errors were obtained by considering the propagation of errors through equations (4) and (5). This analysis, described in detail by Thompson (ref. 10), is similar to that presented by Schotland (ref. 9) The expressions for the uncertainty in $M'_{k,j}$ and $\bar{n}'_k$ are given in equations (6) and (7), respectively, as follows

$$\delta M'_{1,j} = \frac{1}{2(\sigma_{1,1} - \sigma_{1,2})} \left[\frac{(\delta S_{1,J})^2 + (\delta N_1)^2}{(S_{1,J} - N_1)^2} + \frac{(\delta S_{2,J})^2 + (\delta N_2)^2}{(S_{2,J} - N_2)^2} \right]^{1/2} \tag{6}$$

$$\delta \bar{n}'_1 = \frac{1}{\Delta R} \left[(\delta M_{1,j})^2 + (\delta M_{1,j+1})^2 \right]^{1/2} \tag{7}$$

where the uncertainties in $S_{1,j}$ and N_i are given by the equations

$$(\delta S_{1,j})^2 = Q^2 \left[(\delta P_{i,J})^2 + (\delta N_{i,d})^2 + (\delta N_{i,b})^2 \right] + (\delta Q)^2 \left[P_{i,j} + N_{i,d} + N_{i,b} \right]^2 \tag{8}$$

$$(\delta N_i)^2 = Q^2 \left[(\delta N_{i,d})^2 + (\delta N_{i,b})^2 \right] + (\delta Q)^2 \left[N_{i,d} + N_{i,b} \right]^2 \tag{9}$$

and Q has been introduced to represent the electronic amplification which converts received photons to charges stored by the electronic equipment. By assuming that the standard deviation in the laser backscatter and the noise generated by the background are determined by Poisson statistics, equation (6) can be put in the following form:

$$\delta M'_{1,j} = \frac{1}{2(\sigma_{1,1} - \sigma_{1,2})} \left\{ \frac{P_{1,j} + 2(N_{1,d} + N_{1,b})}{P_{1,J}^2} + \frac{P_{2,J} + 2(N_{2,d} + N_{2,b})}{P_{2,J}^2} \right.$$

$$+ \left(\frac{\delta Q}{Q}\right)^2 \left[\frac{(P_{1,J} + N_{1,d} + N_{1,b})^2 + (N_{1,d} + N_{1,b})^2}{P_{1,j}^2} \right.$$

$$\left. \left. + \frac{(P_{2,j} + N_{2,d} + N_{2,b})^2 + (N_{2,d} + N_{2,b})^2}{P_{2,j}^2} \right] \right\}^{1/2} \qquad (10)$$

From the form of equation (10) it is apparent that only the contributions due to shot noise, background and detector noise, and instrument noise have been considered in this analysis. The contributions to $\delta M'_{k,J}$ from uncertainties in transmitted energy, range, variation in backscattering and extinction coefficients due to scintillation effects, and variation in molecular or aerosol content within the field of view have been neglected. The errors in absorption coefficients, laser energy, and range should be small compared to the other sources of uncertainty, whereas the effects of scintillation and variation in backscatter source depend to a large extent on the mode of operation. For example, the time between measuring the backscattered energies from λ_1 and λ_2 and the amount of spatial averaging performed during a regional measurement will, to a great extent, determine the magnitude of these errors. In order to avoid considering such operational problems, it has been assumed that the transmitted wavelengths are either simultaneous or closely spaced in time. (Simultaneous operation would be desirable but would be difficult to implement in an operational system due to the problem of separating the return signals which are closely spaced spectrally.)

In order to consider the performance of a given DAS system based on the criteria discussed, a set of expected backscattered signals for each transmitted wavelength and atmospheric model was calculated as a function of range by using equation (1). Two atmospheric models were used during this simulation, each corresponding to a standard 1962 midlatitude atmosphere (ref. 12) containing a constant ozone concentration of 32 ppb at all altitudes, but contaminated with the SO_2 and aerosol profiles shown in either figure 2 or figure 3. The shape of each SO_2 profile was modeled after an experimentally measured profile (ref. 13) with the ground-level concentration for each case being chosen to represent a range of pollution conditions. The SO_2 profile I (fig. 2(a)) represents a moderately light pollution level with a ground-level concentration of only 37 ppb. (Note that this concentration is well below the level at which SO_2 can be detected by taste, i.e, 0.3 to 0.5 ppm.) The ground-level SO_2

concentration for profile II (fig. 3(a)) is 370 ppb and represents a moderately heavy pollution level, but one which, for hourly averages, has been frequently observed over large cities (ref. 14). Because of the strong correlation between the production of sulfate aerosols and the SO_2 concentration, an effort was made to choose aerosol profiles representative of ones that might be associated with the two SO_2 profiles used here. For example, the horizontal ground-level visibility for aerosol profile I (fig. 2(b)) is approximately 10 km, and represents conditions which might be associated with the SO_2 profile of figure 2(a). The ground-level visibility for aerosol profile II (fig. 3(b)) is approximately 4 km and is one that might be associated with SO_2 profile II (fig. 3(a)).

The following laser line pairs were used in the retrieval of the SO_2 profile 300.05 and 299.30 nm; 298.00 and 299.30 nm, 300.05 and 301.30 nm; 298.00 and 297.40 nm; 296.25 and 297.40 nm. The first wavelength in each of these pairs is the "on" pulse and the second is the "off" pulse. Based on the following considerations, this analysis was restricted to the wavelength region between 296.25 and 301.30 nm. The difference between the SO_2 absorption coefficients for λ_1 and λ_2 is a maximum. The difference between the O_3 absorption coefficients for any pair of λ_1 and λ_2 is, in general, small and at the same time the attenuation due to O_3 absorption is less than for a wavelength lying farther in the ultraviolet. Finally, this spectral region is just under the so-called "ozone umbrella" so that daylight background presents no measurement problems.

The Mie backscattering and extinction coefficients for each scattering cell were determined from an array of normalized backscattering and extinction coefficients associated with a Deirmendjian aerosol haze model M and the assumed vertical distribution of aerosols. The aerosol size distribution for this model is similar to that found in coastal areas (ref. 15). In a similar manner, the attenuation due to O_3 and SO_2 was determined from an array of absorption coefficients and the assumed vertical distribution for each gas. The absorption coefficients for O_3 and SO_2 were obtained from references 16 and 17, respectively, and are given in table I for the wavelengths used in this analysis. Rayleigh backscattering and extinction coefficients were calculated from the following equations (from ref. 18):

$$\beta_r = \left(4.92 \times 10^{-21}\right)\frac{n_m}{\lambda_i^4} \tag{11a}$$

$$\xi_r = \left(4.11 \times 10^{-20}\right)\frac{n_m}{\lambda_i^4} \tag{11b}$$

where n_m was determined from the vertical molecular distribution associated with the standard 1962 midlatitude atmosphere.

In evaluating the expected return signals from equation (1) it was assumed that the backscattered signal from a given range cell could be represented by equation (1) when using backscattering and extinction coefficients that were averaged over the cell. With this in mind, it should be noted that the column content is considered to be from the platform down to the lower edge of the range cell. The average concentration, calculated from the difference between successive column-content values, is associated with the average altitude level between the column-content values. The assignment of these parameters to the altitude levels is illustrated in figure 1.

Table II lists additional parameters that were used to determine the backscattered energy plus noise energy. An effort has been made to use parameters that can be realized by using commercially available technology to characterize a DAS system which could reasonably be expected to be mounted on an aircraft. In formulating such a system the range of laser and receiver parameters that can be considered is, to a large extent, limited. The operational parameters such as platform altitude and range resolution, however, can vary over a large range of values. Those parameters listed in table II represent a combination which provided a reasonable vertical resolution (500 m) while maintaining an uncertainty of less than 20 percent in the retrieval of the column content down to ground level from a single set of laser data.

RESULTS AND DISCUSSION

Results of the retrieval of the SO_2 column content from the platform down to the altitude of a particular scattering cell are shown in figures 4 and 5 Note that in figure 4 the profiles shown in figure 2 were used for the aerosol and SO_2 vertical distribution, whereas figure 5 illustrates the retrieval of SO_2 column content for the SO_2 and aerosol profiles shown in figure 3 The circles represent the "true" column content from the platform down to the scattering cell as calculated from equation (2). The squares in figures 4 and 5 represent the retrieved column content calculated from the simulated return signal by use of equation (4). The uncertainty, indicated by the error bars, is based on a single laser firing for each "on" and "off" wavelength. The inner error bars on the measured data represent the shot noise error, and the outer error bars represent the combination of the shot noise error plus background and detection noise, and a 2-percent instrument error. The triangles indicate the column content that would be calculated if there were no SO_2 in the measurement path. This column content represents the systematic error that would be associated with the particular wavelength pair under consideration.

The qualitative behavior of the random errors considered is, in general, as expected. For example, the shot noise error (inner error bars) increases significantly as the distance from the platform increases. This is due to a decrease in the return signal at the lower altitudes. Consequently, the measurement accuracy tends to be dominated by the shot noise error at the lower altitudes, whereas the instrument error becomes the limiting factor at the

higher altitudes. In figures 5(a) and 5(b) where aerosol profile II and SO_2 profile II are used, the measurement sensitivity is dominated by the shot noise error. For this case there is so little difference between the total and shot noise uncertainty that only one set of error bars can be distinguished. Notice also that in figures 5(a) and 5(b) there is a large increase in the uncertainty between the column-content measurement down to the 625-meter level and the 125-meter level. This uncertainty is due to a relatively large increase in the aerosol concentration at the 1000-meter level which reduces the return signal from levels below 1000 meters.

The measurement accuracy increases as the aerosol concentration decreases and, up to a point, the accuracy improves as the column content increases. This improvement is illustrated in figures 6(a) and 6(b), where the signal-to-noise ratio associated with a measurement of the column content from the aircraft at 2625 m down to the 125-m level is plotted as a function of column content for three line pairs. The signal-to-noise ratio shown in these figures is calculated from a single set of return signals. Aerosol profile I was assumed for figure 6(a), and aerosol profile II was assumed for figure 6(b). The signal-to-noise ratio for all line pairs is higher by a factor of approximately 2 when the aerosol profile I is used. It is interesting to note that the presence of aerosols produces competing effects in that the aerosols cause a stronger backscattered signal while at the same time producing a stronger attenuation. For this reason a signal-to-noise ratio approaching 10 can be achieved even in the presence of aerosol profile II. The pronounced maximum in the signal-to-noise-ratio curves in figures 6(a) and 6(b) is caused by the small difference in the on and off return signal at low column-content values, and a low return in the on signal at the higher column-content values. From figures 6(a) and 6(b) it is also apparent that a slightly higher signal-to-noise ratio occurs for the wavelength pair (i.e., 300.05 and 299.3 nm) having the largest difference in absorption coefficients. As will be shown, this line pair also exhibits a smaller systematic error.

The behavior of the systematic error associated with the column-content measurements for the five wavelength pairs considered is also illustrated by the triangles in figures 4 and 5. This error is due to a difference in the backscattering and attenuation at the two transmitted wavelengths even in the absence of SO_2. The magnitude of this error for the atmospheric conditions assumed for these figures can be as large as the random uncertainty in the measurements. For example, at ground level the systematic correction in figures 4(c) and 4(e) is approximately 18 percent of the true value as compared with a random uncertainty of approximately 17 percent. This comparison is based on a "single shot" retrieval. Signal averaging would tend to reduce the random uncertainty while leaving the systematic correction unchanged and, consequently, would tend to increase the relative importance of the systematic error, particularly for the low SO_2 concentration levels. The wavelength pair having the lowest systematic error is 300.05 and 299.3 nm, and as mentioned previously, this wavelength pair also exhibited the largest signal-to-noise ratio. The lower systematic error for this pair appears to be fortuitous rather than associated with the factors which contributed to the higher signal-to-noise ratio. The major factors contributing to the low systematic error are the relatively small

wavelength separation between the two transmitted wavelengths (i.e., 0.75-nm separation), which reduces the difference in Rayleigh and Mie backscatter and attenuation coefficients, and the relatively small difference in ozone absorption coefficients, which reduces the difference in attenuation due to ozone.

As the SO_2 level increases, the relative significance of the systematic error tends to decrease; this can be seen by comparing figures 4(a) and 5(a). The systematic correction shown in figure 5(a) has been reduced to about 2 percent from the 18 percent in figure 4(a) Note, however, that the ozone profile has not changed, and an increase in the ozone level for the higher SO_2 levels would tend to increase the systematic correction.

The ability of the DAS system assumed here to retrieve SO_2 profiles I and II from a single pair of return signals is illustrated in figures 7 and 8. The measured profile was obtained from the column-content measurements shown in figures 4(a) and 5(a). The uncertainty, as illustrated by the error bars, is related to the uncertainty in the column-content measurements obtained from equation (7). In figure 7 the salient feature to note is that the error in retrieving the vertical distribution of SO_2 is quite large at all altitude levels, whereas in figure 8 the uncertainty becomes unacceptably large only at the lowest altitude. The large error at the lowest level is due in part to the smaller resolution length used in an attempt to get closer to ground level. The large uncertainties in measuring the vertical distribution of SO_2 indicate that, although measurement of the column content to an accuracy of 20 percent or better may be possible on a single shot basis, range-resolved measurements, using the DAS system formulated here, will require averaging over a number of shots. Neglecting the problems associated with averaging a nonhomogeneous horizontal SO_2 distribution and a horizontally varying backscattering source, the uncertainty in an average measurement is inversely proportional to the square root of the number of shots or profiles to be averaged. Figures 9 and 10 illustrate the results of averaging 100 of the profiles shown in figures 7 and 8, respectively, and figure 11 illustrates the results of averaging 100 profiles derived from the column-content data shown in figure 4(c). Note that for a system capable of operating at 30 pulses/sec with simultaneous wavelengths, this would represent a total measurement time of less than 4 seconds. In figures 9 and 11, where SO_2 profile I has been assumed, systematic errors tend to limit the fidelity of the retrieval process. This is particularly true in figure 11, where, except for the lowest altitude level, the difference between the retrieval profile and the true profile is approximately 5×10^{-7} atm-cm/m or 5 ppb. Note that the largest systematic error occurs at the lowest level, which is related to assuming that the ground reflectivity is equal at the two transmitted wavelengths. The magnitude of the systematic error at the lowest level in figure 11 is approximately 2×10^{-6} atm-cm/m or 20 ppb. In figure 9 the corresponding systematic errors are about 9 ppb at the lowest altitude level and about 2 ppb above this level. In figure 10, where SO_2 profile II has been assumed, the relative importance of the systematic error is small and consequently the random error tends to limit the accuracy of the retrieval process to about 10 ppb at the 375-m level and about 84 ppb at the lowest level

CONCLUDING REMARKS

In the preceding analysis, the ability of a differential absorption and scattering (DAS) system to retrieve vertical SO_2 profiles from aircraft altitudes has been studied. The analysis utilized a computer model which simulated "measured" return signals for several different atmospheric conditions. From these measured signals the SO_2 column content from the platform down to various altitude levels and the SO_2 concentration averaged over the vertical resolution of the system were determined and compared to the respective true values as determined from the input profile. Particular care was taken to characterize the DAS system with parameters which could be realized by using commercially available components. Also, the vertical molecular and aerosol profiles which were used to characterize the atmospheric model were chosen to simulate the types of profiles that might be experienced over a large city.

Results of the simulated retrieval were presented for five different line pairs in the spectral region from 296.25 nm to 301.30 nm, an aircraft altitude of 2625 m, and a vertical resolution of 500 m. The fidelity of the retrieval process was determined by considering the systematic and random errors associated with each measurement. The systematic error is due to an inherent difference in the return signals for the two transmitted wavelengths, whereas the random error is due to shot noise in the return signal, background and detector noise, and instrument noise.

Results from this analysis indicate that measurement of SO_2 column content, as well as the vertical distribution of SO_2, from an aircraft platform is well within the capability of the DAS technique. However, it was shown that for a measurement of both the column content and range-resolved concentration, care must be taken in selecting the operating wavelengths to avoid systematic errors larger than the random uncertainty. This was particularly true when low SO_2 levels were to be measured. For moderately high pollution levels, the random uncertainty in the range-resolved concentration measurements tended to limit the fidelity of the retrieval process.

Langley Research Center
National Aeronautics and Space Administration
Hampton, Va. 23665
November 28, 1975

REFERENCES

1. Schotland, R. M.. Some Observations of the Vertical Profile of Water Vapor by Means of a Laser Optical Radar. Proceedings of the Fourth Symposium on Remote Sensing of Environment, Rev. ed., 4864-11-X, Willow Run Lab., Inst. Sci. & Technol., Univ. of Michigan, Dec. 1966, pp 273-283.

2. Schotland, R. M.; Chermack, E. E., and Chang, D. T.: The Measurement of the Vertical Distribution of Water Vapor by the Differential Absorption of Scattered Energy From a Searchlight Beam. Applications, Volume 2 of Humidity and Moisture – Measurement and Control in Science and Industry, Reinhold Pub. Corp., c.1965, pp. 569-582.

3. Rothe, K. W.; Brinkmann, U., and Walther, H.: Applications of Tunable Dye Lasers to Air Pollution Detection· Measurements of Atmospheric NO_2 Concentrations by Differential Absorption Appl. Phys., vol. 3, no. 1, Jan. 1974, pp. 115-119.

4. Grant, W. B.; Hake, R. D., Jr.; Liston, E. M., Robbins, R. C.; and Proctor, E. K., Jr.: Calibrated Remote Measurement of NO_2 Using the Differential-Absorption Backscatter Technique. Appl. Phys. Lett., vol. 24, no. 11, June 1, 1974, pp. 550-552.

5. Grant, W. B., and Hake, R. D., Jr.: Calibrated Remote Measurements of SO_2 and O_3 Using Atmospheric Backscatter. J. Appl. Phys., vol. 46, no. 7, July 1975, pp. 3019-3023.

6. Measures, R. M.: A Comparative Study of Laser Methods of Air Pollution Mapping. UTIAS Rep. No. 174, Univ. of Toronto, Dec. 1971.

7. Ahmed, Samir A.· Molecular Air Pollution Monitoring by Dye Laser Measurement of Differential Absorption of Atmospheric Elastic Backscatter. Appl. Opt., vol. 12, no. 4, Apr. 1973, pp. 901-903.

8. Byer, Robert L.; and Garbuny, Max: Pollutant Detection by Absorption Using Mie Scattering and Topographic Targets as Retroreflectors. Appl. Opt., vol. 12, no. 7, July 1973, pp. 1496-1505.

9. Schotland, Richard M.: Errors in the Lidar Measurement of Atmospheric Gases by Differential Absorption. J. Appl. Meteorol., vol. 13, no. 1, Feb. 1974, pp. 71-77.

10. Thompson, Richard T., Jr.· Differential Absorption and Scattering LIDAR Sensitivity Predictions by Least Squares With Application to Shuttle, Aircraft, and Ground Based Systems. NASA CR-2627, 1976.

11. Wright, M. L.; Proctor, E. K., Gasiorek, L. S.; and Liston, E. M.: A Preliminary Study of Air-Pollution Measurement by Active Remote-Sensing Techniques. NASA CR-132724, 1975.

12. U.S. Standard Atmosphere, 1962. NASA, U.S. Air Force, and U.S. Weather Bur., Dec. 1962.

13. Ludwig, C. B.; Bartle, R.; and Griggs, M.. Study of Air Pollutant Detection by Remote Sensors. NASA CR-1380, 1969.

14. Air Quality Criteria for Sulfur Oxides. NAPCA Publ. AP 50, U.S. Dep. Health, Educ., & Welfare, Jan. 1969. (Available from NTIS as PB 190252.)

15. Deirmendjian, D . Scattering and Polarization Properties of Water Clouds and Hazes in the Visible and Infrared. Appl. Opt., vol. 3, no. 2, Feb. 1964, pp. 187-196.

16. Griggs, M.: Absorption Coefficients of Ozone in the Ultraviolet and Visible Regions. J. Chem. Phys., vol. 49, no. 2, July 15, 1968, pp. 857-859.

17. Thompson, R. T., Jr.; Hoell, J. M., Jr., and Wade, W. R. Measurements of SO_2 Absorption Coefficients Using a Tunable Dye Laser. J. Appl. Phys., vol. 46, no. 7, July 1975, pp. 3040-3043.

18. McCormick, M. P.: Simultaneous Multiple Wavelength Laser Radar Measurements of the Lower Atmosphere. Electro-Optics '71 International Conference, Ind. & Sci. Conf. Management, Inc., c.1971, pp. 495-512.

TABLE I - SO_2 AND O_3 ABSORPTION COEFFICIENTS AT THE WAVELENGTHS USED IN COMPUTER SIMULATION

Wavelength, nm	Absorption coefficient, $(atm\text{-}cm)^{-1}$, for –	
	SO_2	O_3
301.30	6.7	8 7
300.05	32 7	10.0
299.30	7.4	10.9
298.00	27.1	13.0
297.40	8.0	14.3
296.25	28.1	16.6

TABLE II.- PERTINENT PARAMETERS CHARACTERIZING THE COMPUTER SIMULATION OF AN AIRCRAFT-BASED DAS SYSTEM

Platform altitude, m	2625
Cell length, m	500
Telescope area (40.64-cm (16-in.) telescope), m^2	0.129
Transmitted energy, mJ at 0.2 Å bandwidth	0.4
Optical efficiency	0.1
Filter bandwidth, Å	22
Detector noise, counts/sec	20
Background, W/m^2-sr-Å	10^{-6}
Ground reflectivity	0.1
System error, percent	2

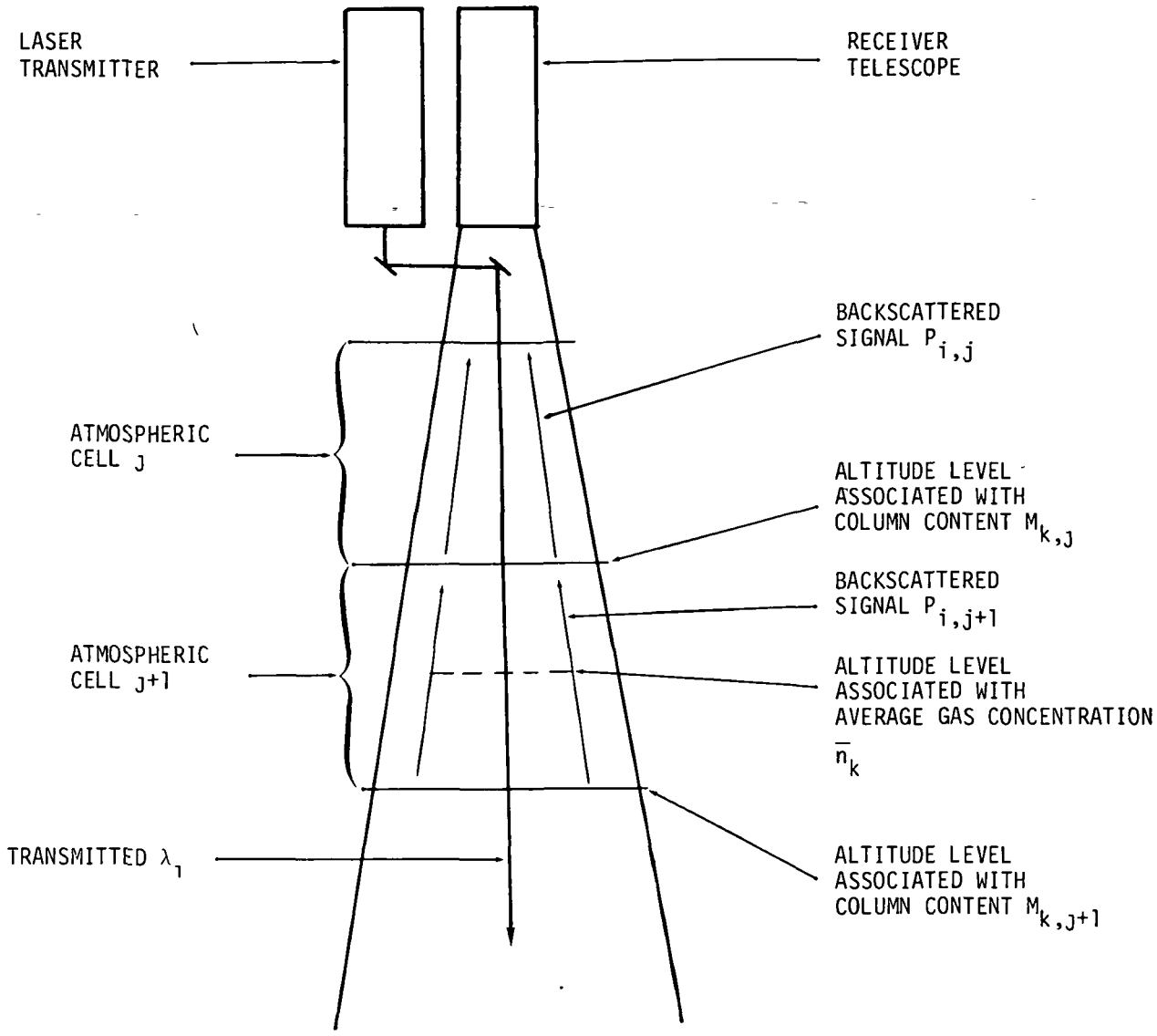

Figure 1.- Illustration of a DAS system, the altitude assignment to the column content, and average gas concentration.

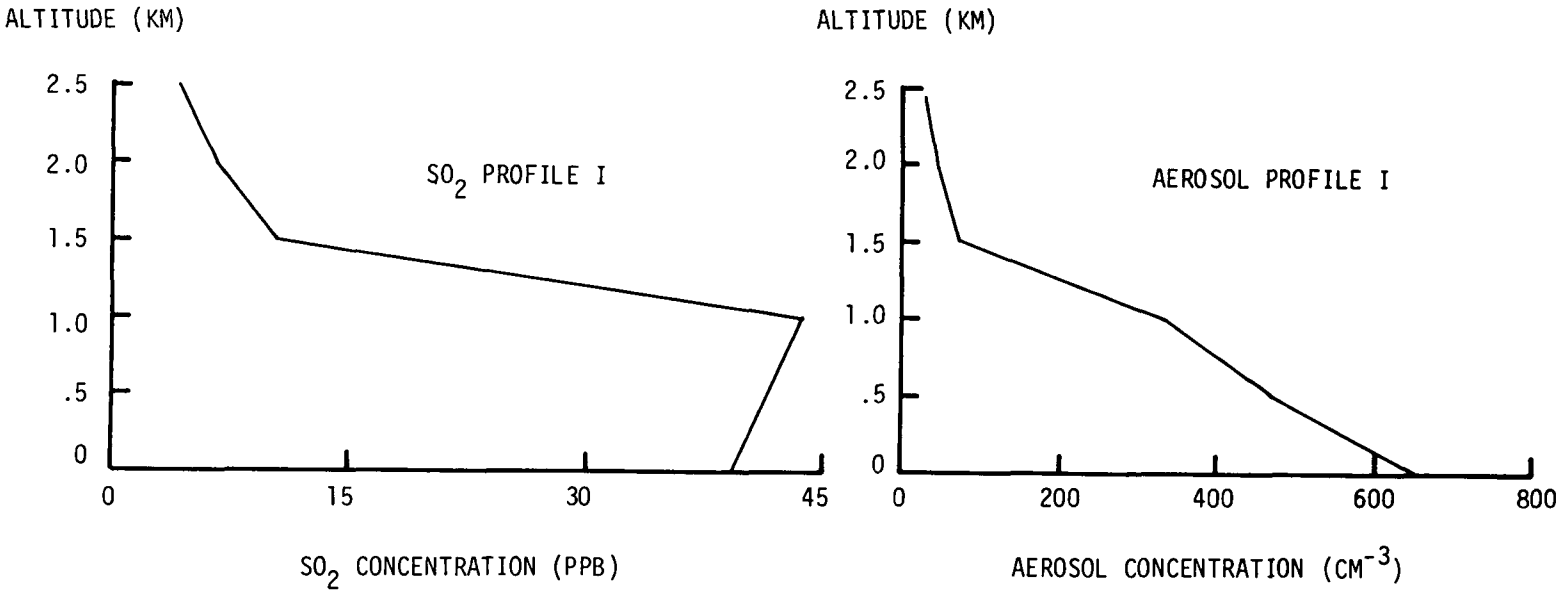

(a) Vertical distribution of SO_2.

(b) Vertical distribution of aerosols.

Figure 2.- Vertical distribution of SO_2 and aerosols used to simulate a moderately light pollution level. Horizontal ground-level visibility is approximately 10 km.

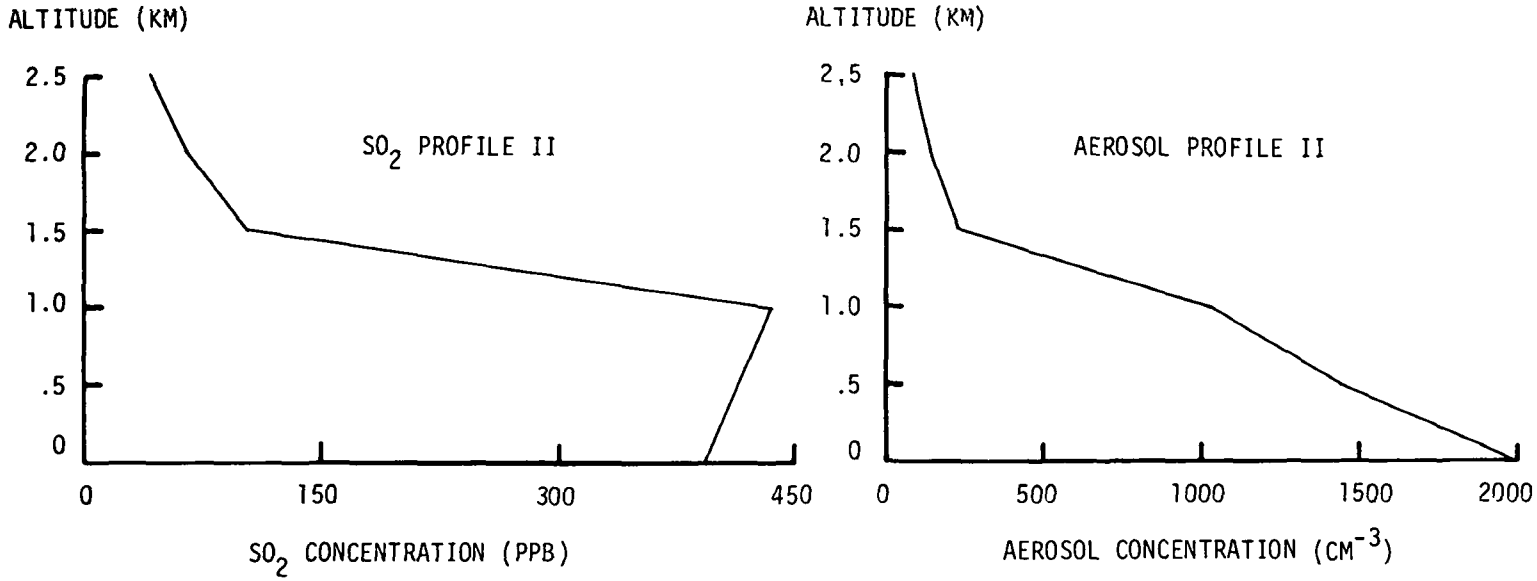

(a) Vertical distribution of SO_2.

(b) Vertical distribution of aerosols.

Figure 3.- Vertical distribution of SO_2 and aerosols used to simulate a moderately heavy pollution level. Horizontal ground-level visibility is approximately 4 km.

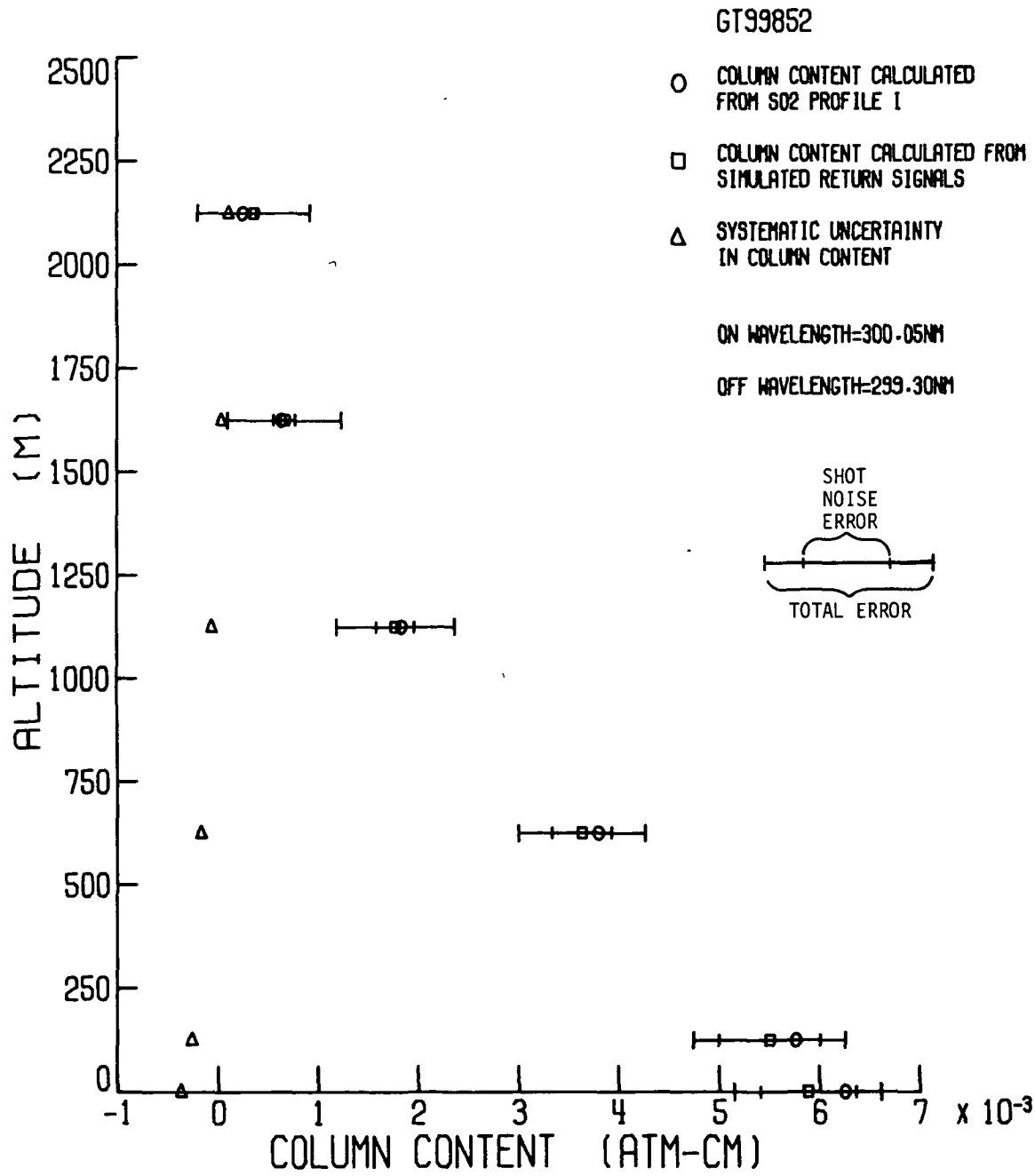

(a) Wavelengths 300.05 and 299.30 nm were used in model.

Figure 4.- Simulated measurement of SO_2 column content from an aircraft platform at 2625 m. Aerosol profile I and SO_2 profile I were used in the atmospheric model.

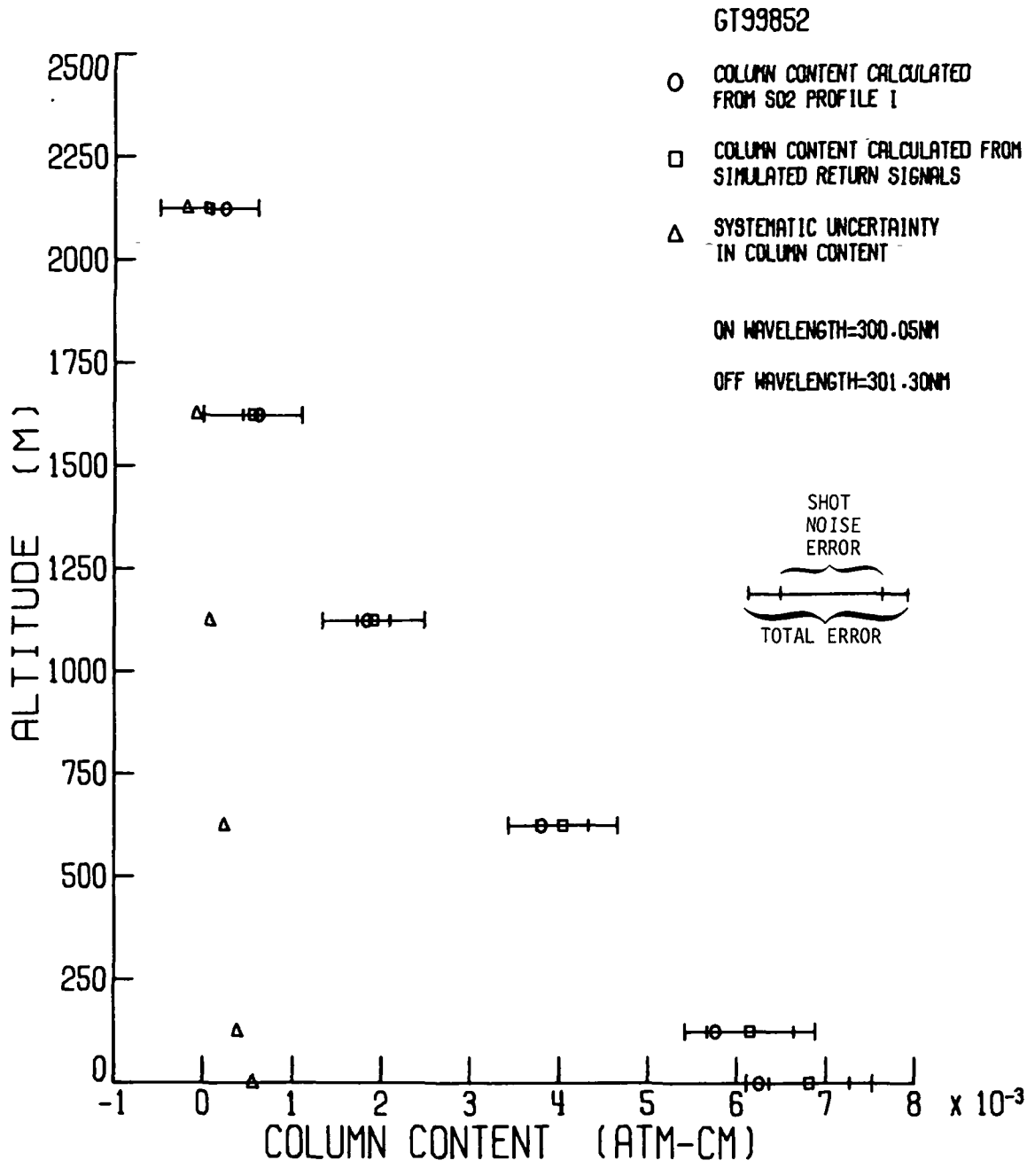

(b) Wavelengths 300.05 and 301.30 nm were used in model.

Figure 4.- Continued.

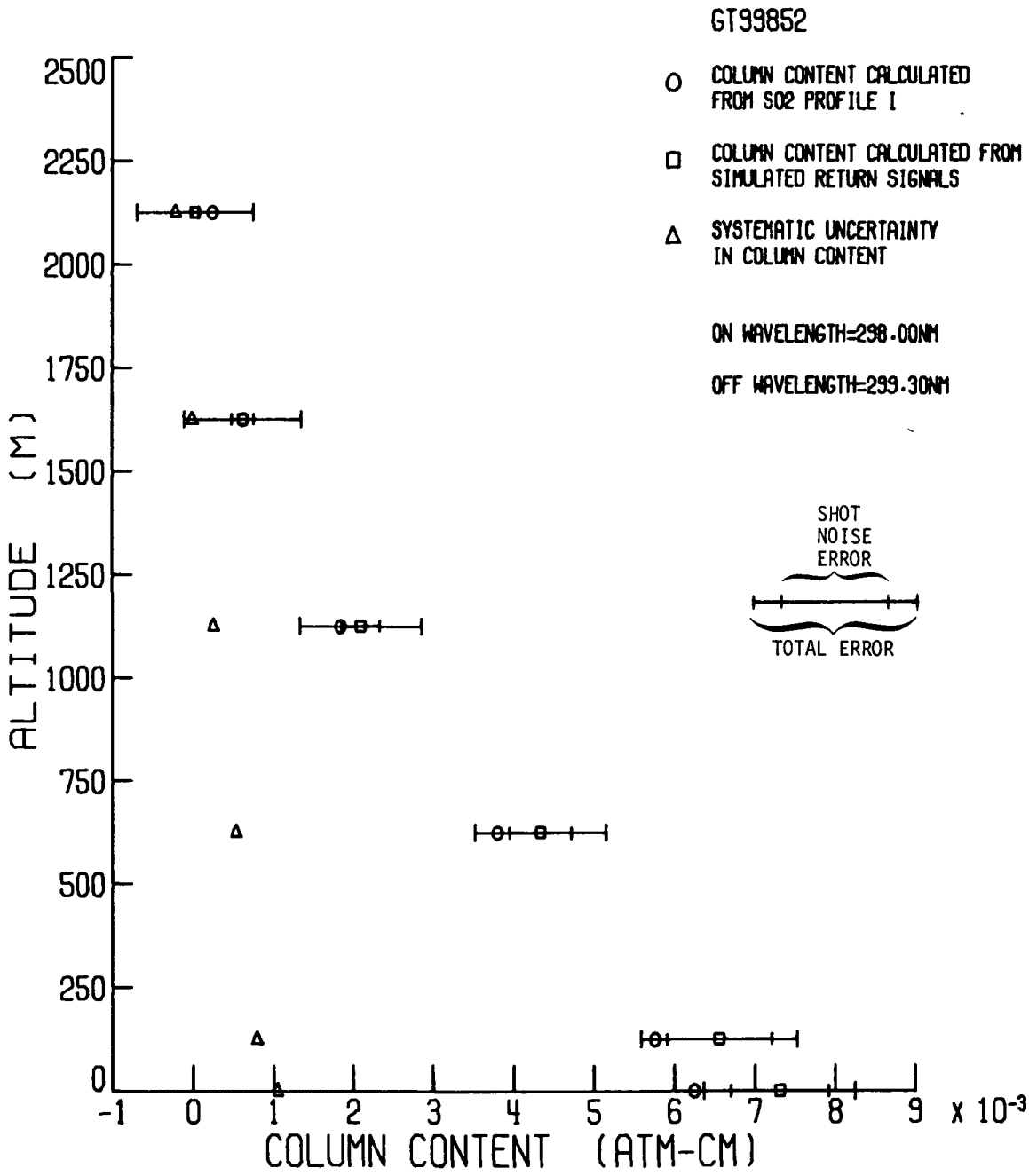

(c) Wavelengths 298.00 and 299.30 nm were used in model.

Figure 4.- Continued.

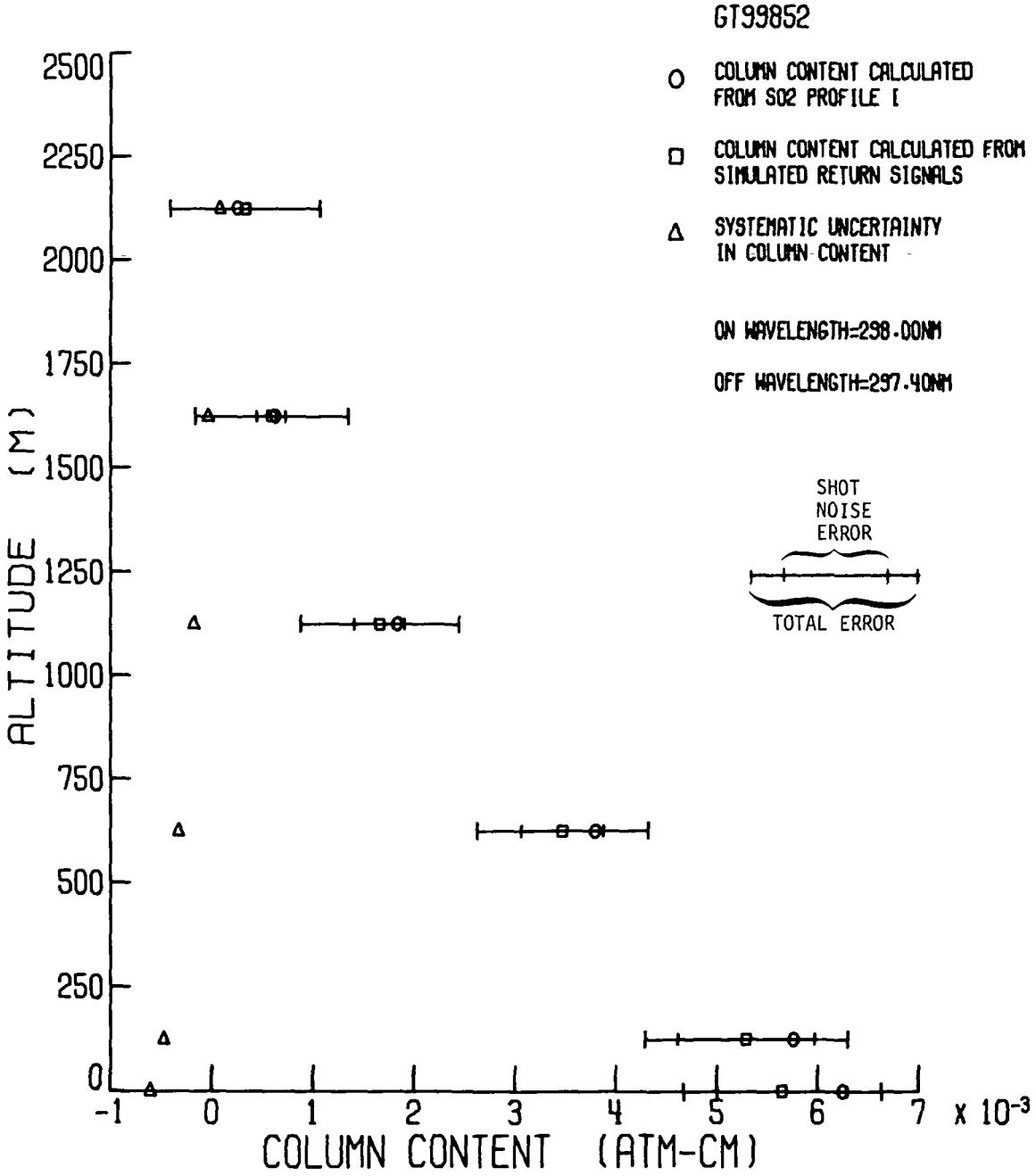

(d) Wavelengths 298.00 and 297.40 nm were used in model.

Figure 4.- Continued.

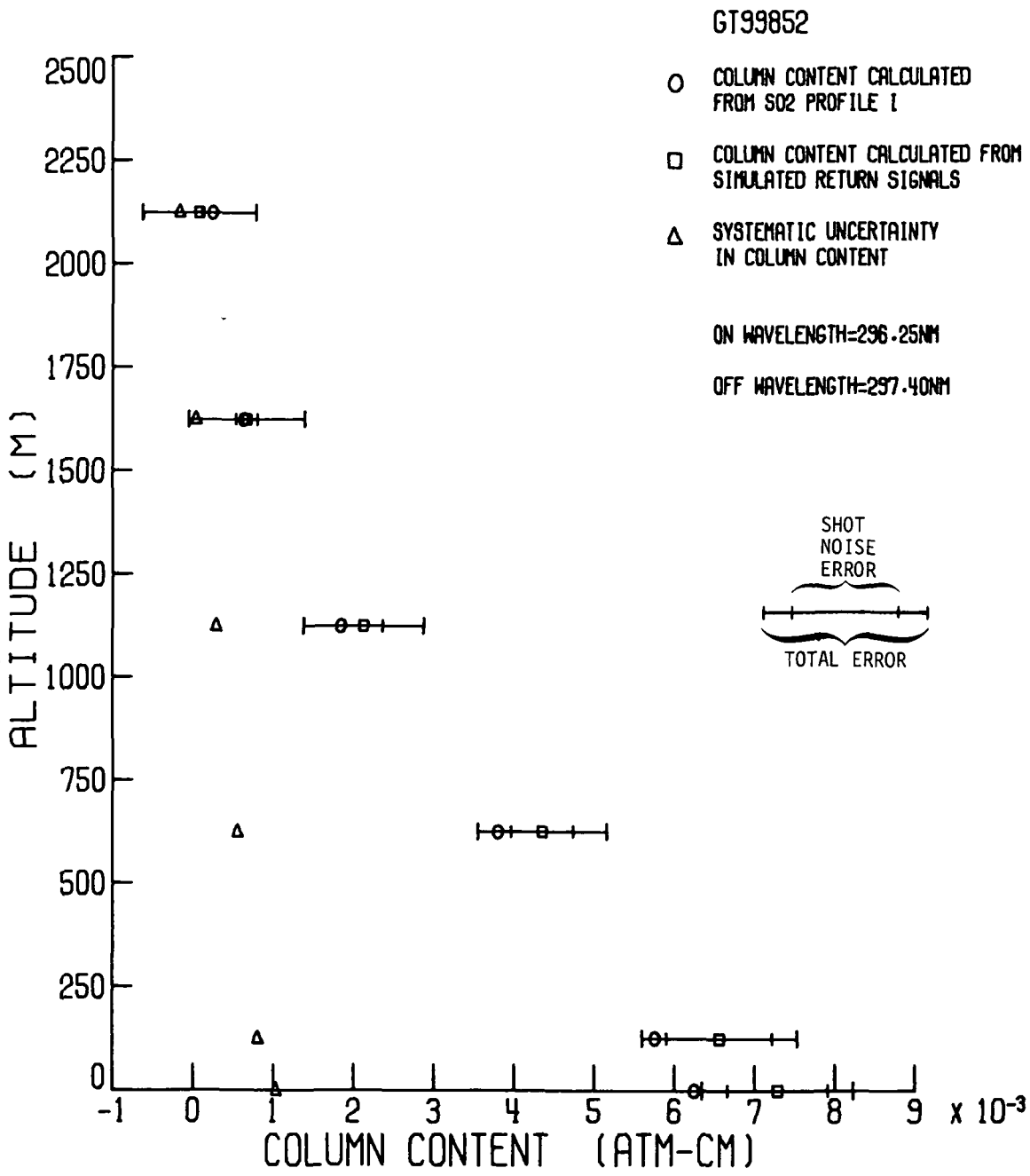

(e) Wavelengths 296.25 and 297.40 nm were used in model.

Figure 4.- Concluded.

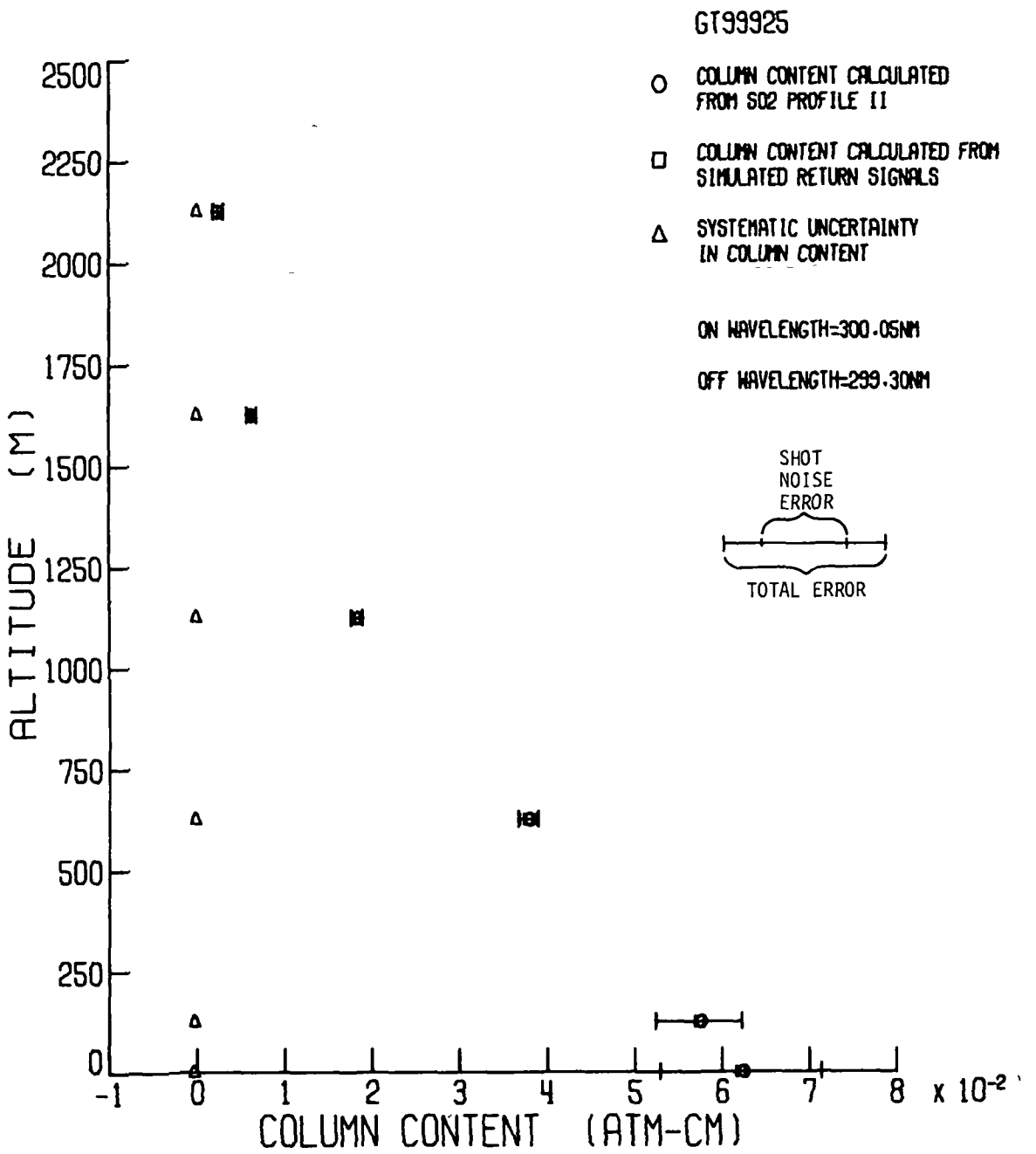

(a) Wavelengths 300.05 and 299.30 nm were used in model.

Figure 5.- Simulated measurement of SO_2 column content from an aircraft platform at 2625 m. Aerosol profile II and SO_2 profile II were used in the atmospheric model.

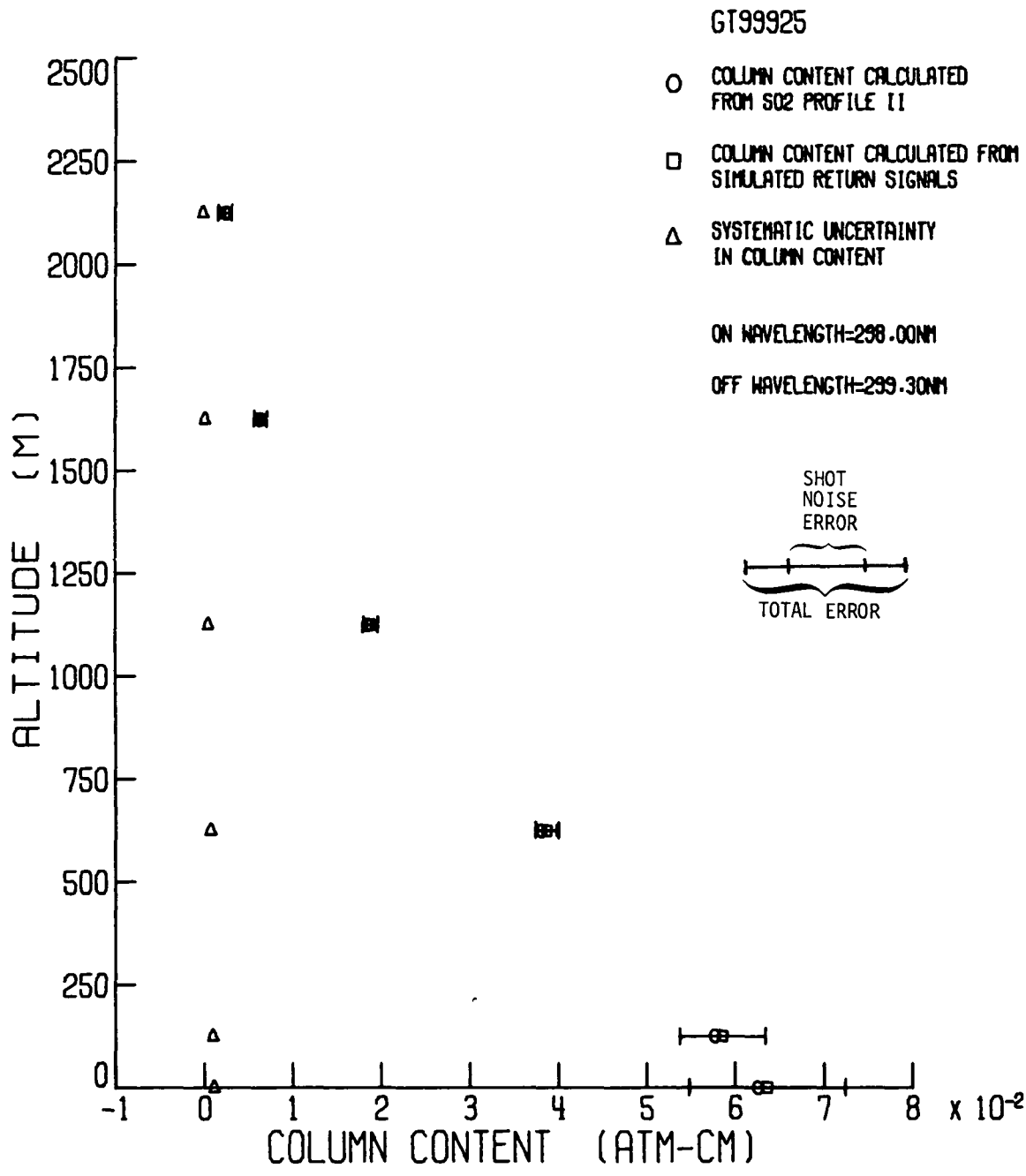

(b) Wavelengths 298.00 and 299.30 nm were used in model.

Figure 5.- Concluded.

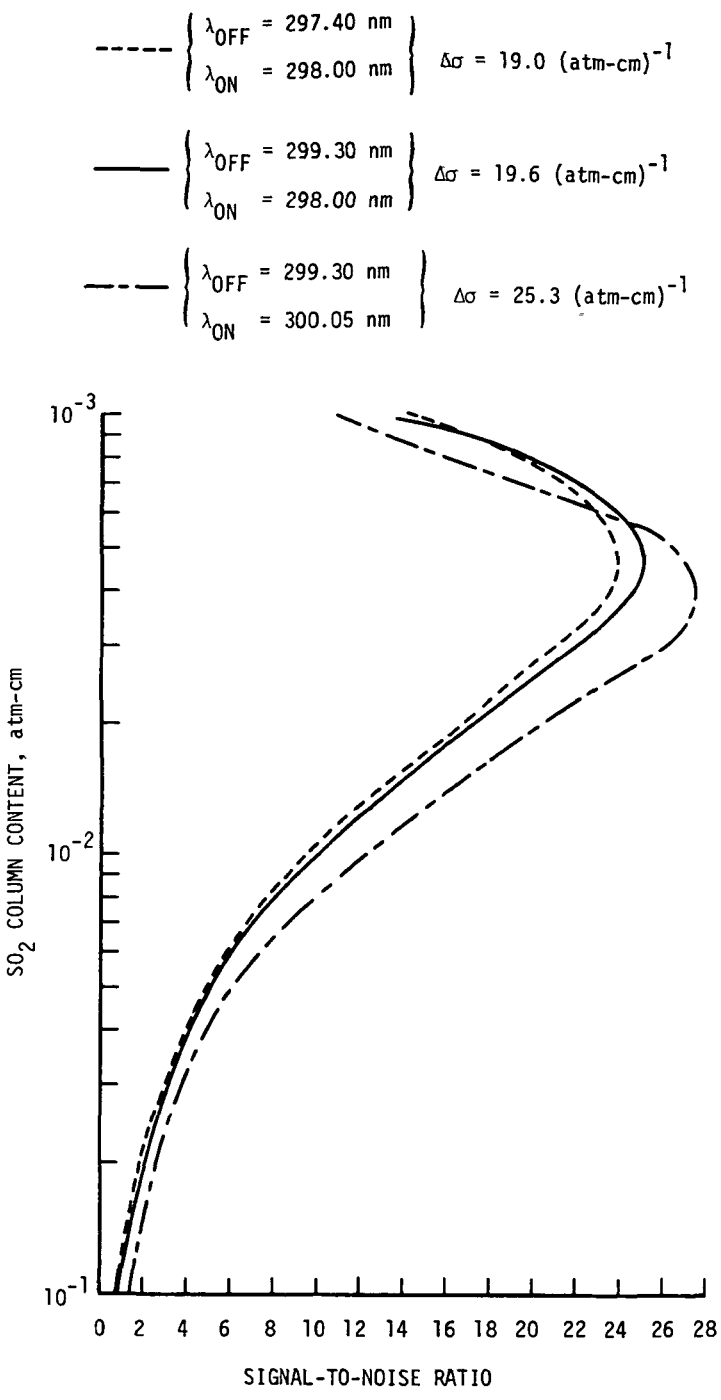

(a) Aerosol profile I was used in atmospheric model.

Figure 6.- The signal-to-noise ratio $\left(M_{k,j}/\delta M_{k,j}\right)$ associated with a measurement of the SO_2 column content from a platform altitude of 2625 m down to the 250-m level.

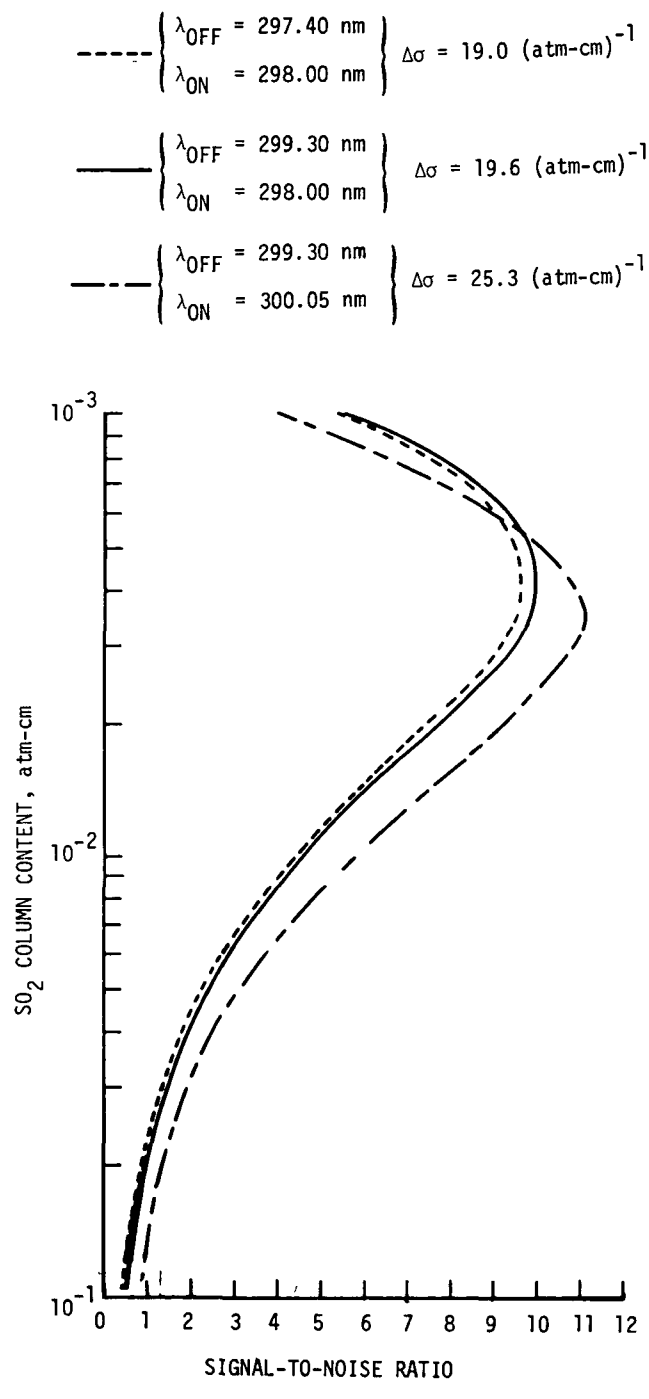

(b) Aerosol profile II was used in atmospheric model.

Figure 6.- Concluded.

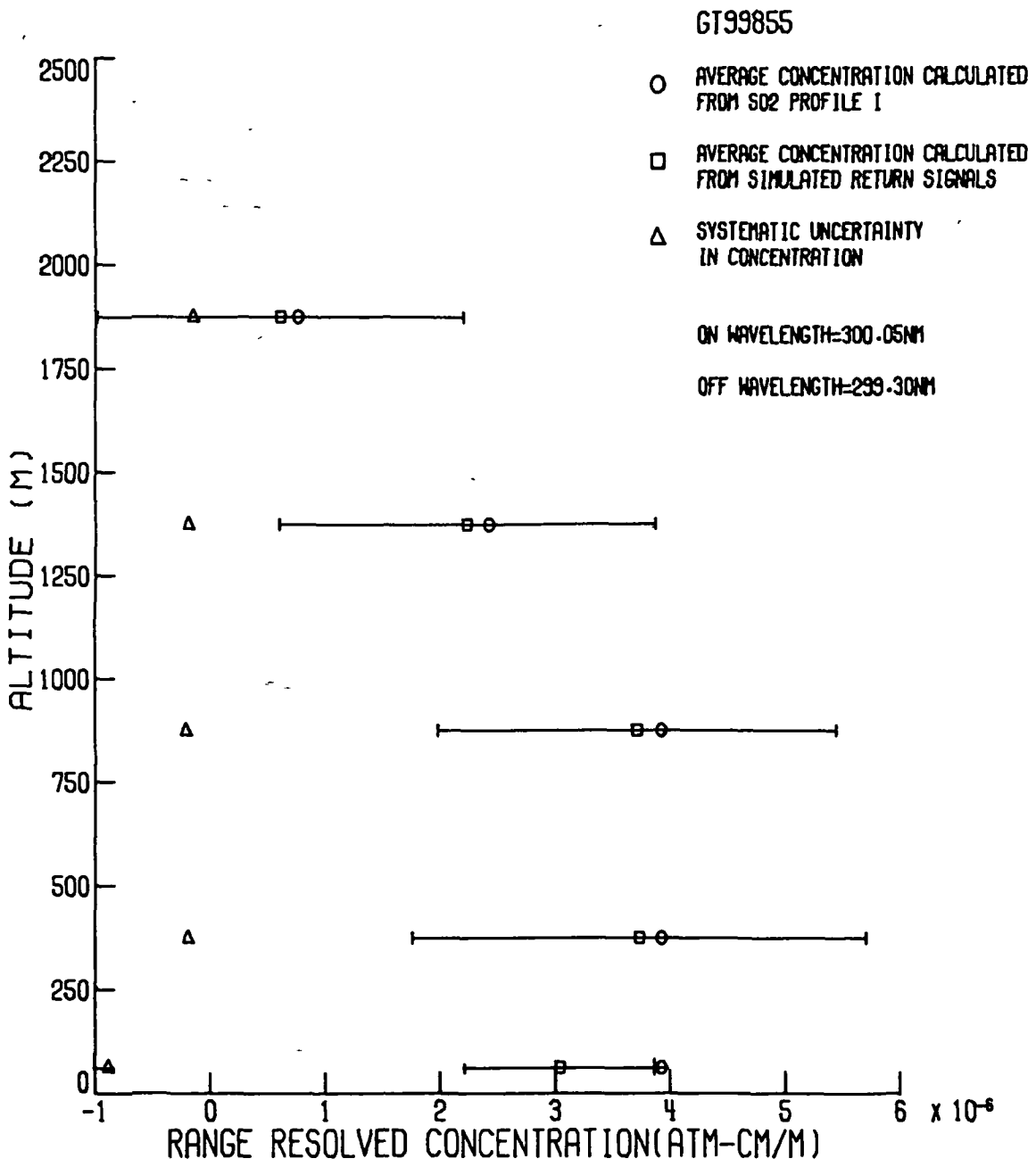

Figure 7.- Retrieval of SO_2 profile I in the presence of aerosol profile I using the wavelength pair 300.05 and 299.30 nm from a platform altitude at 2625 m. The error associated with the measurement at an altitude of 62 m has been scaled in magnitude by a factor of 10.

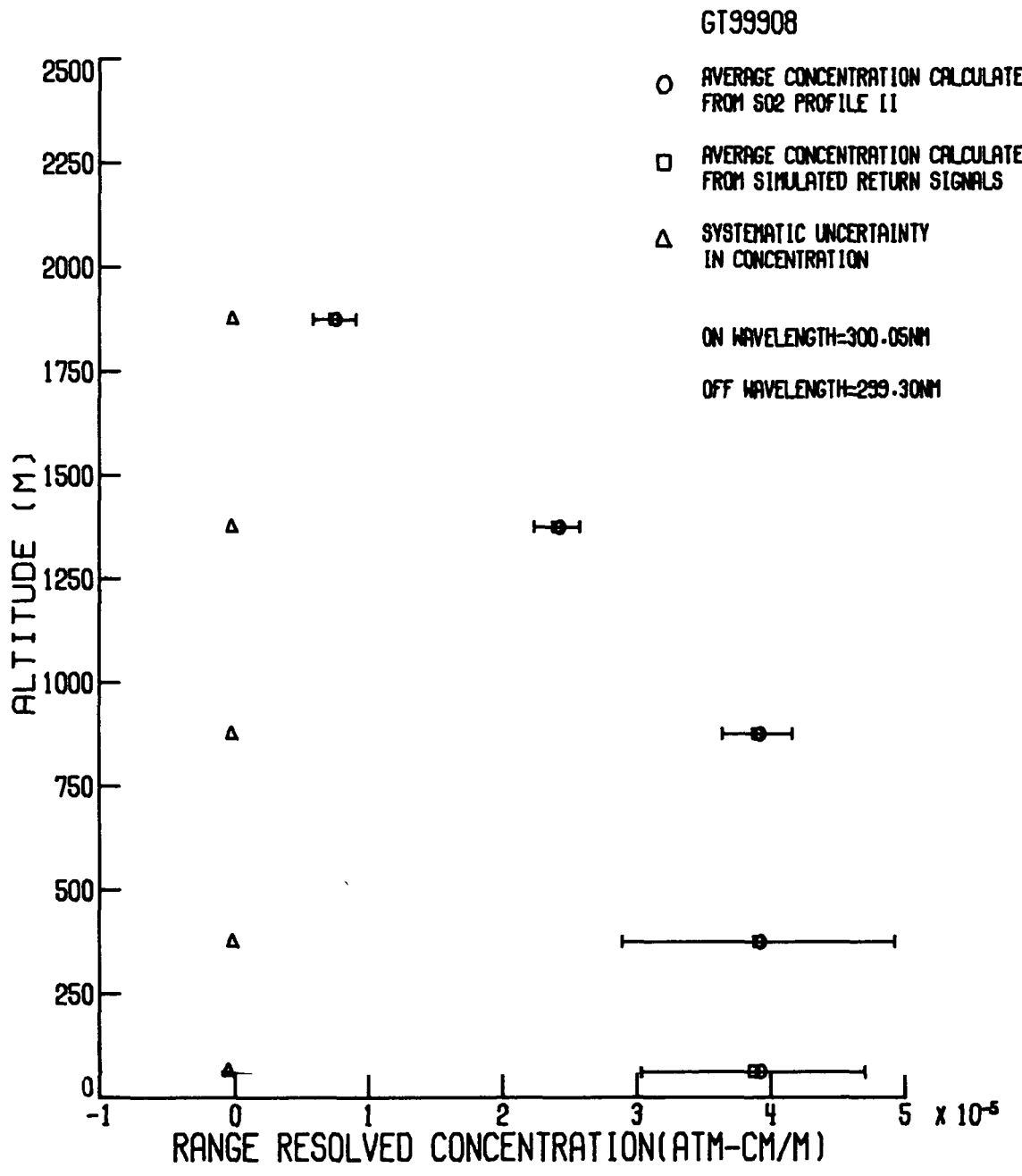

Figure 8.- Retrieval of SO_2 profile II in the presence of aerosol profile II using the wavelength pair 300.05 and 299.30 nm from a platform altitude at 2625 m. The error associated with the measurement at an altitude of 62 m has been scaled in magnitude by a factor of 10.

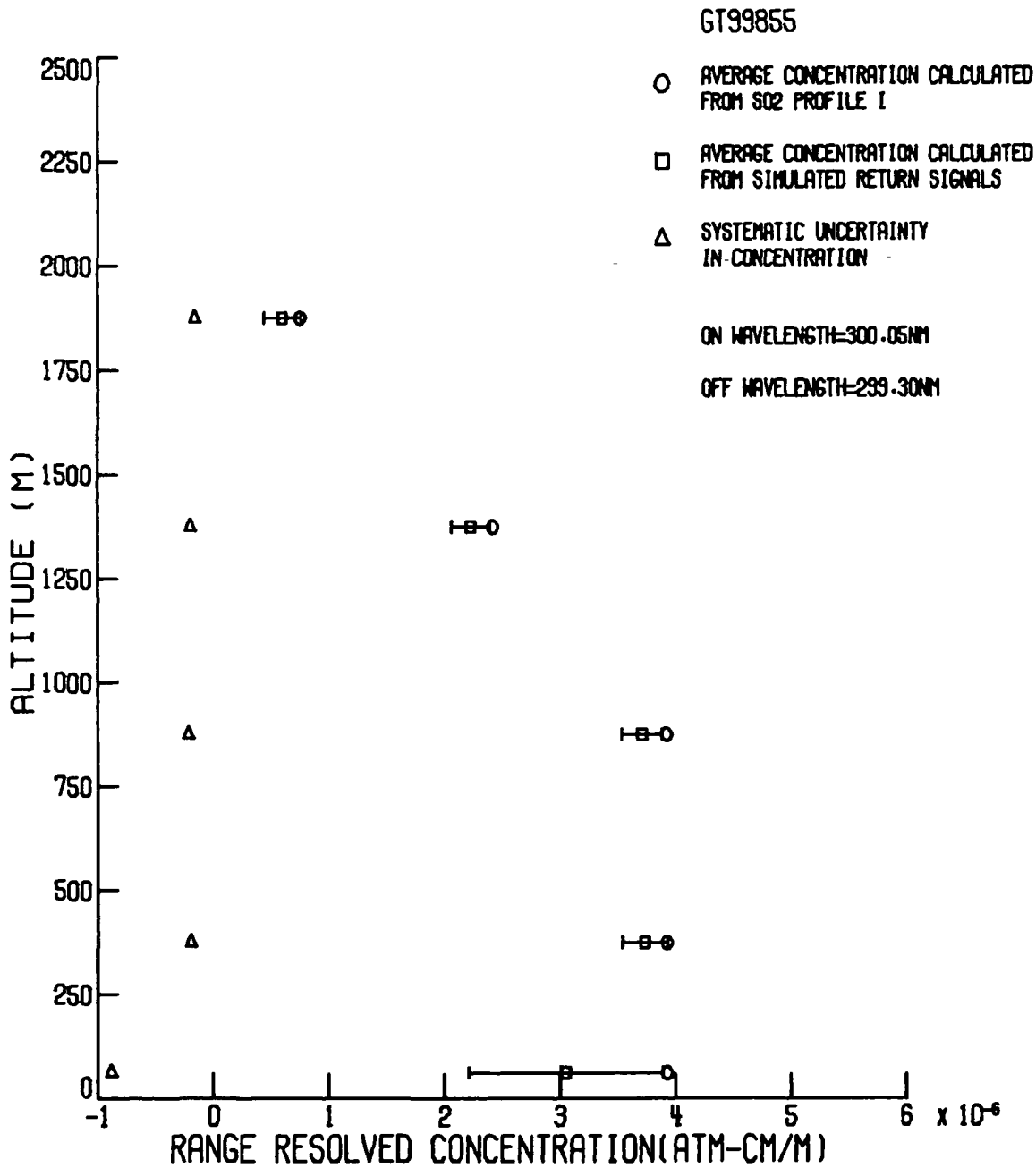

Figure 9.- Retrieval of SO_2 profile I in the presence of aerosol profile I. Retrieval accuracy has been improved by averaging 100 of the single shot retrievals shown in figure 7.

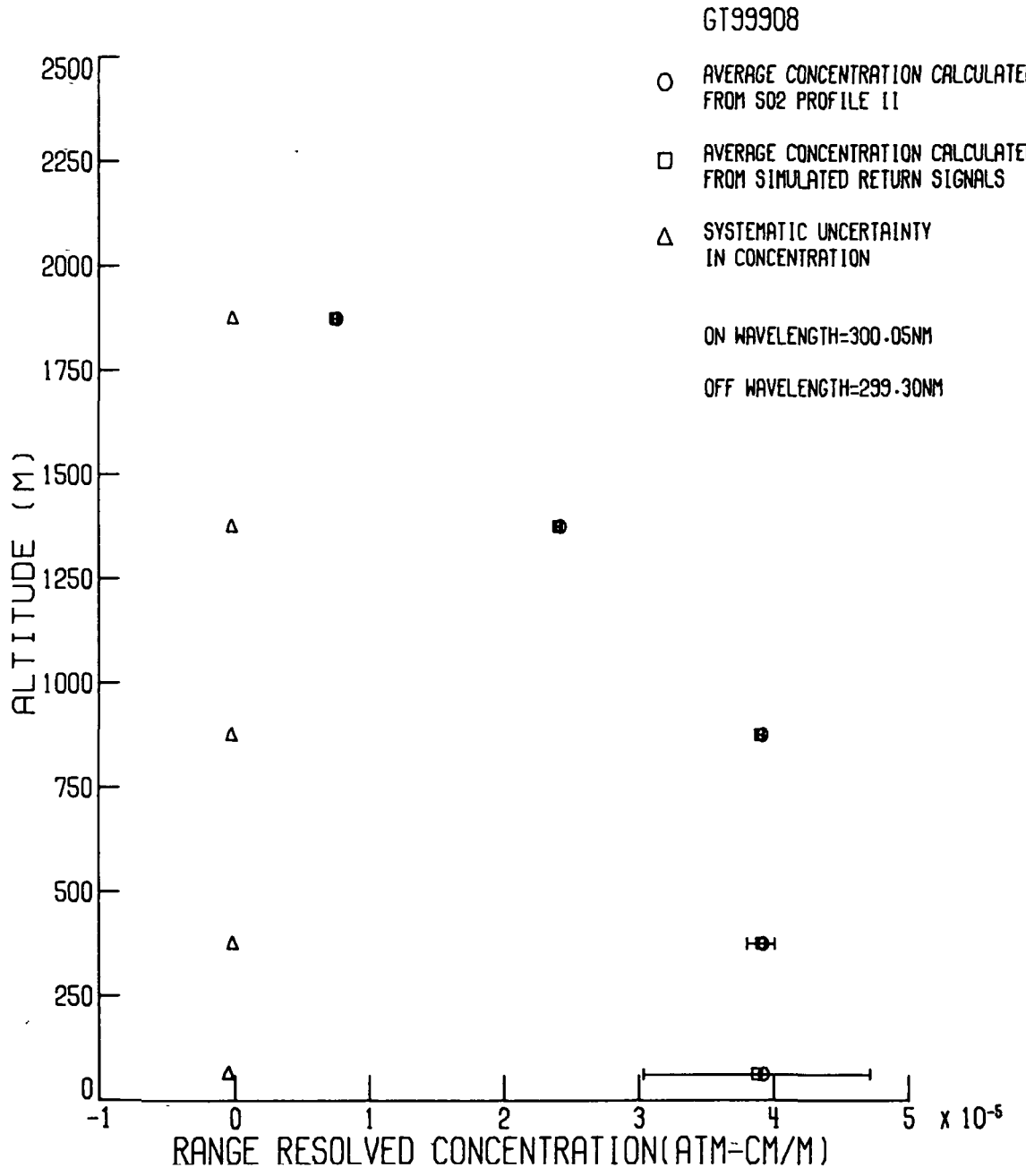

Figure 10.- Retrieval of SO_2 profile II in the presence of aerosol profile II. Retrieval accuracy has been improved by averaging 100 of the single shot retrievals shown in figure 8.

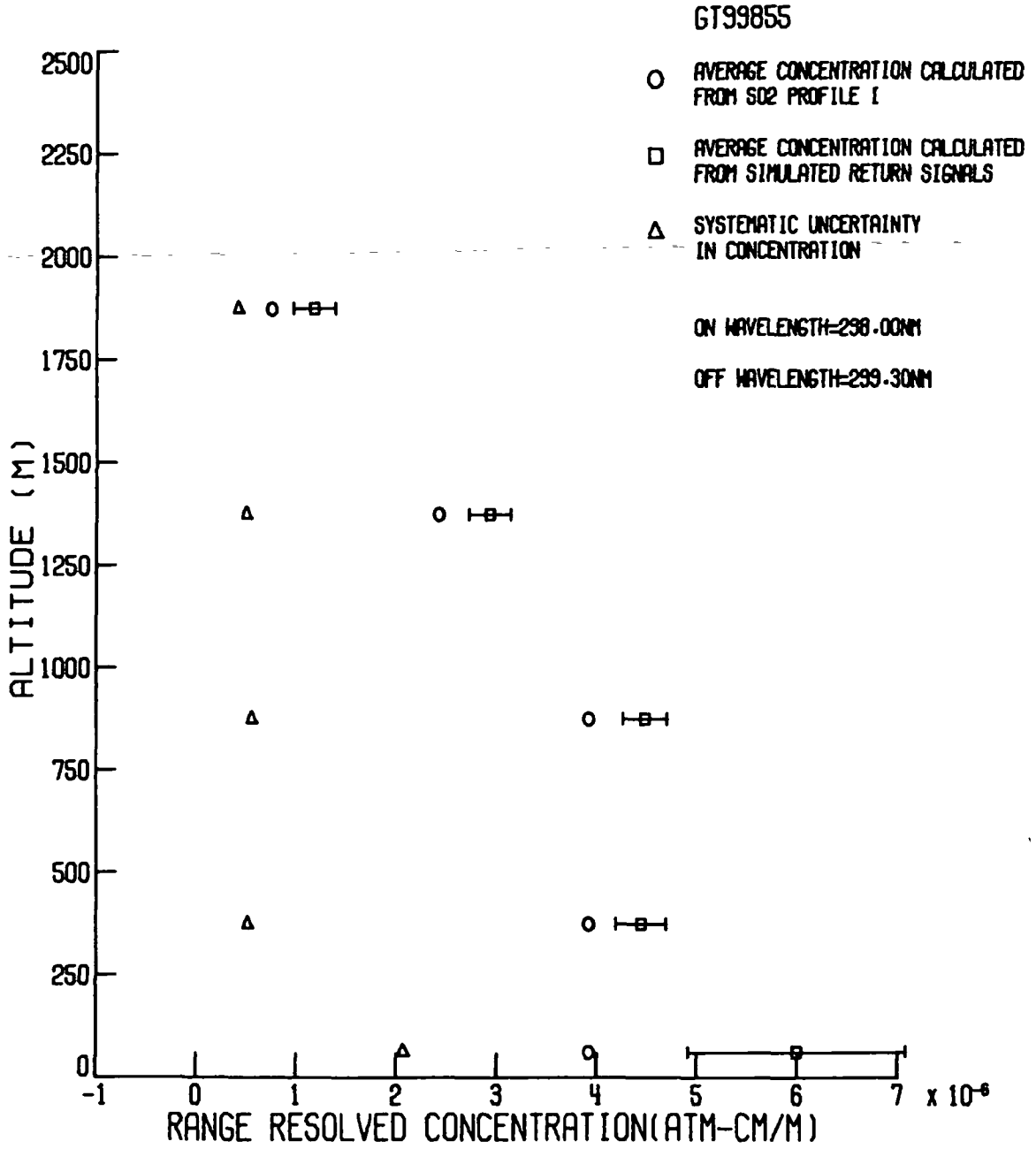

Figure 11.- Retrieval of SO_2 profile I in the presence of aerosol profile I after averaging 100 single shot retrievals. Wavelengths 298.00 and 299.30 nm were used.

"The aeronautical and space activities of the United States shall be conducted so as to contribute . to the expansion of human knowledge of phenomena in the atmosphere and space. The Administration shall provide for the widest practicable and appropriate dissemination of information concerning its activities and the results thereof"

—NATIONAL AERONAUTICS AND SPACE ACT OF 1958

NASA SCIENTIFIC AND TECHNICAL PUBLICATIONS

TECHNICAL REPORTS Scientific and technical information considered important, complete, and a lasting contribution to existing knowledge

TECHNICAL NOTES Information less broad in scope but nevertheless of importance as a contribution to existing knowledge

TECHNICAL MEMORANDUMS Information receiving limited distribution because of preliminary data, security classification, or other reasons Also includes conference proceedings with either limited or unlimited distribution.

CONTRACTOR REPORTS Scientific and technical information generated under a NASA contract or grant and considered an important contribution to existing knowledge

TECHNICAL TRANSLATIONS. Information published in a foreign language considered to merit NASA distribution in English.

SPECIAL PUBLICATIONS Information derived from or of value to NASA activities Publications include final reports of major projects, monographs, data compilations, handbooks, sourcebooks, and special bibliographies

TECHNOLOGY UTILIZATION PUBLICATIONS Information on technology used by NASA that may be of particular interest in commercial and other non-aerospace applications Publications include Tech Briefs, Technology Utilization Reports and Technology Surveys

Details on the availability of these publications may be obtained from:

SCIENTIFIC AND TECHNICAL INFORMATION OFFICE

NATIONAL AERONAUTICS AND SPACE ADMINISTRATION

Washington, D.C. 20546